Joint Coding–Precoding With Low-Complexity Turbo-Decoding

Zhengdao Wang, *Member, IEEE*, Shengli Zhou, *Member, IEEE*, and Georgios B. Giannakis, *Fellow, IEEE*

***Abstract*—We combine error-control coding with linear precoding (LP) for flat-fading channels, as well as for wireless orthogonal frequency-division multiplexing transmissions through frequency-selective fading channels. The performance is analyzed and compared with the corresponding error-control-coded system without precoding. By wedding LP with conventional error-control coding, the diversity order becomes equal to the error-control code's minimum Hamming distance times the precoder size. We also derive a low-complexity turbo-decoding algorithm for joint coded–precoded transmissions. We analyze the decoding complexity and compare it with an error-control-coded system without LP. Extensive simulations with convolutional and turbo codes for HiperLan/2 channels support the analysis and demonstrate superior performance of the proposed system.**

***Index Terms*—Coding, diversity, fading, HiperLan, linear precoding (LP), orthogonal frequency-division multiplexing (OFDM).**

I. Introduction

In WIRELESS mobile communications, the channel is often time-varying due to relative transmitter–receiver motion and multipath propagation. Such a time-variation is commonly referred to as fading, which impairs system performance severely. When the data rate is high in relation to the channel bandwidth, multipath propagation becomes also frequency-selective and causes intersymbol interference (ISI). By implementing inverse fast Fourier transform (IFFT) at the transmitter and fast Fourier transform (FFT) at the receiver, orthogonal frequency-division multiplexing (OFDM) converts an ISI channel into a set of parallel ISI-free subchannels with gains equal to the channel's frequency response values on the FFT grid. The cyclic prefix, which is inserted before each transmitted block and is removed from each received block, eliminates the interblock interference that is induced by the ISI channel.

Manuscript received December 13, 2001; revised October 30, 2002; accepted March 19, 2003. The editor coordinating the review of this paper and approving it for publication is A. F. Molisch. This work was supported by the National Science Foundation (NSF) Wireless Initiative Grant 99-79443, by the NSF Grant 01-0516, and by the U.S. Army Research Laboratory (ARL) under the Collaborative Technology Alliance (CTA) Program, Cooperative Agreement DAAD DAAD 19-01-2-011. This paper was presented in part at the IEEE Vehicular Technology Conference, Birmingham, AL, May 2002, and at the European Wireless Conference, Florence, Italy, February 2002.

Z. Wang is with the Department of Electrical and Computer Engineering, Iowa State University, Ames, IA 50011 USA (e-mail: zhengdao@iastate.edu).

S. Zhou is with the Department of Electrical and Computer Engineering, University of Connecticut, Storrs, CT 06269 USA (e-mail: shengli@engr.uconn.edu).

G. B. Giannakis is with the Department of Electrical and Computer Engineering, University of Minnesota, Minneapolis, MN 55455 USA (e-mail: georgios@ece.umn.edu).

Digital Object Identifier 10.1109/TWC.2004.827770

OFDM affords simple channel equalization because it renders the ISI channel equivalent to a number of single-tap ISI-free subchannels, and thus, only a one-tap division is needed to equalize each subchannel. Without error-control (EC) coding, OFDM transmissions are decoded reliably only when the channel does not experience deep fades (frequency nulls), or when the transmitter has channel state information (CSI) so that the subchannels with deep fades are excluded from carrying information.

To mitigate fading effects, whether frequency-flat or frequency-selective, practical wireless systems often employ some form of coding. Examples of popular EC schemes include block codes (e.g., Reed–Solomon or Bose–Chaudhuri–Hocquenghem) [5], convolutional codes (CCs) [11], [12], Trellis or coset codes [28], and turbo-codes (TCs) [12], [14]. Some of them also require CSI at the transmitter [19], [21], which may be unrealistic or too costly to acquire in wireless applications where the channel changes on a constant basis.

Diversity is an important counter-measure against fading, and comes in different flavors, including frequency, time, and space. Diversity manifests itself in the average system performance as the asymptotic slope of the error-rate versus signal-to-noise ratio (SNR) curve in a log–log scale (asymptotic in SNR). Large diversity order is, therefore, desired for high performance. EC coding can achieve certain order of diversity. But to increase diversity, an increase in decoding complexity is usually necessary. For example, with convolutional coding, diversity increase leads to an exponential increase in decoding complexity, as we will assert in the paper.

A recent flavor of diversity is the so-called *signal space diversity* that is realized by linear precoding (LP) [4], [31]. With LP alone, maximum multipath-diversity is achieved at the price of (possibly exponentially) increased complexity. Therefore, from the decoding complexity perspective, only small-size precoders should be used.

In this paper, we combine Galois field EC coding and complex field LP with small size precoders (for low complexity) to improve system performance, mainly in terms of the diversity gain. The original contributions of this paper are as follows:

1) derivation of a concatenated coding–precoding scheme with bit-interleaving at the transmitter for frequency-selective channels with OFDM, and also for frequency-flat channels with single-carrier transmissions;
2) performance analysis of the proposed scheme in fading channels using pairwise error probability (PEP) techniques, to establish that the concatenation offers multiplicative diversity order;

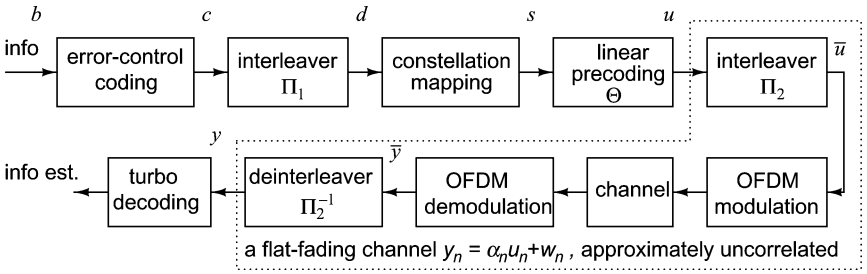

Fig. 1. System block diagram.

3) development of an iterative decoding algorithm for the joint coding–precoding scheme with a complexity only a few times that of an EC-coded system without precoding. When EC coding or LP is used alone, the same amount of increase in complexity will only allow for a much smaller increase in diversity order (as compared to the multiplicative diversity).

II. Joint Coded-Precoded Transmissions

We consider two types of transmissions through time-varying (fading) channels: frequency-selective and frequency-flat. With OFDM and sufficient interleaving, the former can be described by the same model as the latter, which enables a unified design and analysis for multicarrier and single-carrier systems. Application of our joint coding–precoding approach to either system leads to improved performance.

A. OFDM Transmissions Through Frequency-Selective Channels

Fig. 1 depicts the coded and linearly precoded OFDM system under consideration. A stream of information bits[1] b is first encoded using EC coding—we will mainly focus on CCs and TCs, but other codes are also applicable. The coded symbols, denoted by c, go through the interleaver Π_1 that outputs permuted symbols denoted by $d = \Pi_1[c]$. The symbols d are mapped to constellation symbols s. We let $\mathcal{A}$ denote the constellation alphabet, and $|\mathcal{A}|$ its size. Every $\log_2|\mathcal{A}|$ consecutive symbol of d is mapped to one constellation symbol when d is binary. Possible constellations include binary phase-shift keying (BPSK), quadrature phase-shift keying (QPSK), and M-ary quadrature amplitude modulation (QAM). When the constellation is multilevel, i.e., $|\mathcal{A}| > 2$, the constellation bit mapping policy will affect the performance, depending on the detection scheme. For conventional noniterative decoding, Gray mapping is usually optimum; if iterative bit-demapping is used, anti-Gray mapping outperforms Gray-mapping [24]. For bit mapping optimization according to mutual information criteria, we refer the reader to [24]. Constellation mapping will affect our system performance in the form of coding gain. We henceforth assume that the mapping has been optimized according to [24].

After constellation mapping, successive blocks of M symbols $\mathbf{s}_i := [s_{iM}, s_{iM+1}, \ldots, s_{iM+M-1}]^T$ are linearly precoded by a matrix $\mathbf{\Theta}$ of size $M \times M$, and a precoded block $\mathbf{u}_i = \mathbf{\Theta}\mathbf{s}_i$ is, thus, obtained. The block size M is a design parameter. Each block $\mathbf{u}_i$ is serialized to $u_{iM}, u_{iM+1}, \ldots, u_{iM+M-1}$. The precoded symbols u are interleaved by a second interleaver Π_2, whose role is to decorrelate the channel in the frequency domain. With a sufficiently increased size, Π_2 can also decorrelate the channel in the time domain, although this can be achieved equally well by increasing the size of Π_1. The output of Π_2, denoted by $\bar{u}_n = \Pi_2[u_n]$, is passed on to the "OFDM modulator," which includes serial-to-parallel conversion to blocks of size N (the OFDM symbol size), IFFT, and cyclic prefix insertion; see, e.g., [12], [30]. The resulting output is serialized for transmission. The main difference[2] of our transmitter model from a coded OFDM system such as HiperLan [11] is the presence of the linear precoder $\mathbf{\Theta}$, and the interleaver Π_1, whose roles will be clarified in the next subsection. The design of the interleavers will be discussed in Section III-C.

We will deal with slowly varying and generally frequency-selective channels. We will model the symbol-rate sampled channel at baseband as a finite impulse response (FIR) filter of order L with impulse response $h[n] = \sum_{l=0}^{L} h_l \delta[n-l]$, where h_l are slowly varying channel taps modeled as wide-sense stationary random processes. The frequency response of the channel is denoted as $H(f) := \sum_{l=0}^{L} h_l e^{-j2\pi f l}$. We will adopt for each tap a complex Gaussian distribution of zero-mean with equal-variance real and imaginary parts; i.e., each h_l obeys the Rayleigh fading model. The channel variation is slow enough so that: 1) $h[n]$ remains approximately invariant within one OFDM symbol and 2) reliable estimation of $h[n]$ is possible. Although the channel remains constant over one OFDM symbol, we allow it to vary from OFDM symbol to OFDM symbol according to Jakes' fading model. We will also suppose that perfect channel information and synchronization have been acquired at the receiver.

The receiver first performs "OFDM demodulation" by discarding the cyclic prefix per block to form the received OFDM symbols (which are blocks of size N) that are subsequently FFT processed. The lth resulting sample $\bar{y}_{(k-1)N+l}$ in the kth demodulated OFDM symbol can be written as (see, e.g., [30])

$$\bar{y}_{(k-1)N+l} = H\left(\frac{l}{N}\right)\bar{u}_{(k-1)N+l} + \bar{\eta}_{(k-1)N+l}, \quad l \in [0, N-1], \quad k = 0, 1, \ldots \tag{1}$$

where $\bar{\eta}$ is the FFT processed additive white Gaussian noise (AWGN). The variance of the noise is $N_0/2$ per real dimension.

[1]We use letters b, c, d, s, u, y, and η with no subscript to denote sequences; e.g., $b = (\ldots, b_{-1}, b_0, b_1, \ldots)$.

[2]Other differences such as pilot symbols and guard bands in HiperLan are not essential to our discussion.

Since the FFT is a linear transform, the frequency response variates $\{H(l/N) : l \in [0, N-1]\}$ are also complex Gaussian. Although the FFT is an orthogonal transformation, if $N > L+1$, the N variates are correlated even though the $(L+1)$ impulse response taps are independent. If we define $y_n := \Pi_2^{-1}[\bar{y}_n]$, $\eta_n := \Pi_2^{-1}[\bar{\eta}_n]$, and $\alpha_n := \Pi_2^{-1}[H((n \bmod N)/N)]$, then the deinterleaved version of (1) can be expressed as

$$y_n = \alpha_n u_n + \eta_n. \tag{2}$$

With a well designed Π_2 of large enough size, the correlation between α_n's can be greatly reduced. In the performance analysis of Section III, we will assume the idealized case where α_n's are uncorrelated Gaussian random variables with zero-mean. Their variance will be normalized to one by dividing each α_n by the ensemble average of the channel energy. The effect of residual correlation will be examined mainly via computer simulations.

B. Single-Carrier Transmissions Through Frequency-Flat Channels

It is important to emphasize that (2) corresponds also to the input–output relationship of a single-carrier transmission through a flat-fading channel, where the block diagram of Fig. 1 is still valid without the OFDM modulator–demodulator. From the theoretical point of view, multicarrier transmissions with OFDM and single-carrier transmissions over frequency-flat channels are both examples of ISI-free transmissions. The joint coding–precoding idea and results of this paper are directly applicable to both.

C. LP for Signal Space Diversity

The notion of signal space diversity was originally introduced for flat-fading Rayleigh channels [4]. The idea in our setup, that allows also for frequency-selective fading, is to rotate the M-dimensional vectors $\mathbf{s}_i \in \mathcal{A}^M$ using a unitary matrix $\mathbf{\Theta}$ so that the resulting signal set $\mathcal{U} := \{\mathbf{u} : \mathbf{u} = \mathbf{\Theta}\mathbf{s}, \mathbf{s} \in \mathcal{A}^M\}$ possesses the following *full diversity property*:

$$\forall \mathbf{s}_i, \mathbf{s}_i' \in \mathcal{A}^M, \quad \text{if } \mathbf{s}_i \neq \mathbf{s}_i', \quad \text{then } [\mathbf{\Theta}\mathbf{s}_i]_k \neq [\mathbf{\Theta}\mathbf{s}_i']_k\,,\ \forall k \in [1, M] \tag{3}$$

where $[\cdot]_k$ denotes the kth entry of a vector. In words, for two distinct blocks, their precoded (rotated) counterparts are different in *all* their components. With this property, if each component $[\mathbf{u}_i]_k$ of a rotated block $\mathbf{u}_i$ goes through a fading channel, and is, thus, scaled by an independent fading coefficient α_n, then as long as one of the M coefficients α_n is not too small, one can uniquely detect $\mathbf{s}_i$ from the rotated vectors $\mathbf{u}_i = \mathbf{\Theta}\mathbf{s}_i$. This signal space diversity has been exploited recently with multiantenna transmissions in [6], [33], and with uncoded OFDM in [16].

Suppose now that the precoded symbols $\mathbf{\Theta}\mathbf{s}_i$ pass through an ISI-free fading channel modeled as in (2). Using Chernoff bounding techniques, we can approximate the probability of block errors $P_E : P(\mathbf{u}_i \to \mathbf{u}_j, i \neq j)$, by [31], [33]

$$P_E \approx (G_c \cdot \mathrm{SNR})^{-G_d} \tag{4}$$

where the *diversity gain* G_d is the minimum Hamming distance between the linearly precoded vectors $\mathbf{u}_i, \mathbf{u}_j \in \mathcal{U}$; i.e., recalling that $|\{\cdot\}|$ denotes the cardinality of a set, we have

$$G_d = \min_{\mathbf{u}_i \neq \mathbf{u}_j} |\{k : [\mathbf{u}_i]_k \neq [\mathbf{u}_j]_k\}|\,.$$

Note that G_d determines the slope of the error rate versus an appropriately defined SNR curve, while the *coding gain* G_c in (4) measures savings in SNR as compared to a fictitious system with error rate given by $(1/\mathrm{SNR})^{G_d}$. Both G_d and G_c depend on the choice of $\mathbf{\Theta}$, and naturally a full (maximum) diversity is indeed achieved by precoders satisfying the full diversity property (3) [31], [33].

As pointed out in [4] and [16], signal space diversity offers a bandwidth-efficient countermeasure against fading in the sense that it does not reduce the transmission rate. We call our matrix $\mathbf{\Theta}$ a linear precoder because it implements a linear transformation, and in order to enable full signal space diversity, it does not have to be unitary as originally required by [4]. However, there are indeed good reasons that motivate unitary precoders (UPs).

1) A UP $\mathbf{\Theta}$ does not change the Euclidean distances between the M-dimensional vectors $\{\mathbf{s}_i\}$, and hence unitary precoding does not alter performance when the channel is purely AWGN (with no fading);
2) For certain sizes M, the "best" precoders in terms of maximizing diversity and coding gains turn out to be almost always unitary [33].

Henceforth, we will focus on UPs, and the resulting OFDM system with UP will be abbreviated as UP-OFDM.

D. Merits of Combining LP With Coding

Given the documented success of EC coding and the merits of LP in the presence of fading, we here combine their strengths. LP alone can achieve a diversity of order M with a well-designed precoder $\mathbf{\Theta}$ over a fast flat-fading channel [4], [33]. In the limit $(M \to \infty)$, the $M \times M$ precoder $\mathbf{\Theta}$ converts a Rayleigh fading channel to an AWGN channel [4]. The price paid is twofold. First, to collect full diversity gains, maximum likelihood (ML) decoding is needed. ML decoding is an NP-hard problem, although the universal lattice decoder (a.k.a., sphere decoder) can approach ML performance in polynomial time [26]. Therefore, LP enables large diversity at high decoding complexity. Second, since the ideal linear precoder with $M \to \infty$ renders the fading channel equivalent to an AWGN one, its performance is limited by that of an uncoded transmission in AWGN.

Motivated by the need to reduce the ML decoding complexity of LP, we will only use small precoders of size $M \leq 4$. We will later see that there is practically little to be gained by using precoders of size $M > 4$. For $M \leq 4$ and small size constellations such as BPSK or QPSK, one can even afford an exhaustive ML search for decoding.

For $M = 2$ and $M = 4$, the following precoders have been shown to enable full diversity and maximum coding gain of 1 and 1/2, respectively, for QAM constellations [13], [16], [33]

$$\mathbf{\Theta}_2 = \frac{1}{\sqrt{2}} \begin{bmatrix} 1 & e^{j\frac{\pi}{4}} \\ 1 & e^{j\frac{5\pi}{4}} \end{bmatrix} \tag{5}$$

$$\mathbf{\Theta}_4 = \frac{1}{2} \begin{bmatrix} 1 & e^{j\frac{\pi}{8}} & e^{j\frac{2\pi}{8}} & e^{j\frac{3\pi}{8}} \\ 1 & e^{j\frac{5\pi}{8}} & e^{j\frac{10\pi}{8}} & e^{j\frac{15\pi}{8}} \\ 1 & e^{j\frac{9\pi}{8}} & e^{j\frac{18\pi}{8}} & e^{j\frac{27\pi}{8}} \\ 1 & e^{j\frac{13\pi}{8}} & e^{j\frac{26\pi}{8}} & e^{j\frac{39\pi}{8}} \end{bmatrix}. \tag{6}$$

Two nice properties of these precoders are that they enable maximum coding and diversity gains, while all their entries have equal norm $|\theta_{k,m}| = 1/\sqrt{M}, \forall k, m \in [0, M-1]$. The latter will be useful when deriving the performance of coded UP-OFDM.

Unlike LP, EC coding is capable of achieving large coding gains even when the channel is AWGN. When used over Rayleigh fading channels, coding is also capable of offering diversity gains. For example, a linear block code with minimum Hamming distance $d_{\min}$ incurs the following codeword error probability in Rayleigh fading [32, p. 526]

$$P_E \approx \frac{1}{2} A_{d_{\min}} \left(2\frac{E_s}{N_0} \right)^{-d_{\min}} \tag{7}$$

where E_s denotes energy per coded symbol, and $A_{d_{\min}}$ is the number of codewords of weight $d_{\min}$. We deduce from the exponent in (7) that the diversity gain of the code is $d_{\min}$. For CCs, the diversity gain equals d_{free}, the free-distance of the code. For an (n, k) CC with memory m, the free distance is upper bounded by [32, p. 575]

$$d_{\text{free}} \leq (m+1)n. \tag{8}$$

Therefore, for fixed n, the free distance can only increase at the price of increasing the memory m. However, such a diversity increase, which is at best linear in the memory m, will result in an exponential increase in decoding complexity, because the number of trellis states is 2^m for binary codes.

Wedding LP with EC coding offers *multiplicative* increase in diversity: The overall diversity will be the product of the individual diversity orders, as we will show in Section III. Interestingly, the iterative (or turbo) decoding in Section IV will only be a few times more complex than the sum of their individual complexities.

III. Performance Analysis

In this section, we will study the performance of our coded–precoded system supposing ML decoding at the receiver. Our major tool will be the union bound. We will only treat convolutional coding here, but our analysis carries over to any linear code, including block and TCs, with slight modifications (e.g., by replacing d_{free} by $d_{\min}$).

We start with the bit-error enumerating function $B(Z)$ of the EC code used in Fig. 1: $B(Z) = \sum_{w=d_{\text{free}}}^{\infty} B_w Z^w$, where B_w is the total number of nonzero information bits on the weight-w error events. Using $B(Z)$ and PEP analysis, the bit-error rate (BER) will be upper bounded using union bound techniques [1]. We will analyze the PEP first.

Let δ denote the minimum Euclidean distance between the constellation points: $\delta := \min\{|s_1 - s_2| : s_1, s_2 \in \mathcal{A}, s_1 \neq s_2\}$. Clearly, δ depends on the constellation used, and the energy per coded symbol E_s. We invoke the following simplifying approximations in order to make the PEP analysis tractable.

- A1) The EC-coded bits are mapped to different constellation symbols.
- A2) The constellation symbols are separated by at least δ.
- A3) The constellation symbols of an error event are precoded into different precoded blocks.

A1 and A3 are approximately true, thanks to interleaver Π_1, especially for small weight error events, or when the size of Π_1 is large. We can call them perfect interleaving assumptions. A2 is true by definition, but we will use it to relax our upper bound on PEP.

A. PEP

Consider that the coded sequence $\tilde{\mathbf{c}} = (\ldots, \tilde{c}_{-1}, \tilde{c}_0, \tilde{c}_1, \ldots)$ is to be interleaved, mapped to constellation symbols, and linearly precoded before transmission. Let $\mathbf{c} = (\ldots, c_{-1}, c_0, c_1, \ldots)$ be another coded sequence of Hamming distance w away from $\tilde{\mathbf{c}}$. When convolutionally coded, $\mathbf{c}$ will have a trellis path that diverges from the path of $\tilde{\mathbf{c}}$ and remerges back to it (we assume that the code is not catastrophic). Thanks to the interleaver Π_1, the symbols in $\mathbf{c}$ that are different from $\tilde{\mathbf{c}}$, say $c_{j_1}, c_{j_2}, \ldots c_{j_w}, 1 \leq j_1, j_2, \ldots, j_w < \infty$, will be scattered after interleaving and mapped to different constellation symbols, say $s_{n_1}, s_{n_2}, \ldots, s_{n_w}$. For small w's, by designing the interleaver Π_1, the symbol indexes $n_1, n_2, \ldots, n_w$ can be guaranteed to be separated by at least M, i.e., $|n_a - n_b| > M, \forall a, b \in [1, w], a \neq b$; hence, the constellation symbols $s_{n_1}, s_{n_2}, \ldots, s_{n_w}$ will enter different blocks $\mathbf{s}_{i_1}, \mathbf{s}_{i_2}, \ldots, \mathbf{s}_{i_w}$. Let $m_a := n_a \bmod M$ denote the column index of $\mathbf{\Theta}$ that s_{n_a} will be multiplied with, and define $l_a := n_a - m_a$, where $a \in [1, w]$.

All the symbols in $\{s_n\}$ except s_{n_a}, $a \in [1, w]$, will be the same as their corresponding symbols $\{\tilde{s}_n\}$ in the sequence $\tilde{\mathbf{c}}$. If we subtract the received sample $\tilde{y}_n$, which corresponds to $\tilde{\mathbf{c}}$, from y_n, which corresponds to $\mathbf{c}$, we will obtain [c.f. (2)]

$$\Delta y_{l_a+k} = \alpha_{l_a+k} \theta_{k,m_a} \Delta s_{n_a}, \quad a = 1, 2, \ldots, w, \qquad k = 0, 1, \ldots, M-1 \tag{9}$$

where $\Delta y_n := y_n - \tilde{y}_n$, and $\Delta s_n := s_n - \tilde{s}_n$. For $n \neq l_a + k$, we have $\Delta y_n = 0$.

The PEP $P_E(\tilde{\mathbf{c}} \to \mathbf{c}|h)$ conditioned on the channel h (h is a generic symbol denoting the entire channel realization) is determined by the squared Euclidean distance

$$d^2(y, \tilde{y}) = \sum_{a=1}^{w} \sum_{k=0}^{M-1} |\alpha_{l_a+k} \theta_{k,m_a} \Delta s_{n_a}|^2. \tag{10}$$

By definition of δ, it is true that $|\Delta s_{n_a}| \geq \delta$. Since all entries of $\mathbf{\Theta}$ have equal norm $1/\sqrt{M}$, it follows that

$d^2(y,\tilde{y}) \geq (\delta^2/M)\sum_{a=1}^{w}\sum_{k=0}^{M-1}|\alpha_{l_a+k}|^2$. Therefore, the PEP can be upper bounded by

$$P(\tilde{\mathbf{c}} \to \mathbf{c}|h) \leq Q\left(\sqrt{\frac{\left(\frac{\delta^2}{M}\right)\sum_{a=1}^{w}\sum_{k=0}^{M-1}|\alpha_{l_a+k}|^2}{2N_0}}\right) \quad (11)$$

where $Q(x) := \int_x^\infty (2\pi)^{-1/2}\exp(-x^2/2)dx$.

Using the Chernoff bound $Q(x) \leq (1/2)\mathrm{e}^{-x^2/2}$, and averaging with respect to the complex Gaussian distribution of the α's, we obtain

$$P(\tilde{\mathbf{c}} \to \mathbf{c}) \leq \frac{1}{2}\left(1+\frac{\left(\frac{\delta^2}{M}\right)}{4N_0}\right)^{-wM}. \quad (12)$$

Equation (12) shows that a diversity of order wM is achieved for the PEP.

B. Bit Error Probability

Applying the union bound to all error events, we can bound the BER as [1, p. 718]

$$P_b \leq \sum_{w=d_{\text{free}}}^{\infty}\frac{1}{2}B_w\left(1+\frac{\left(\frac{\delta^2}{M}\right)}{4N_0}\right)^{-wM} = \frac{1}{2}B\left(\left(1+\frac{\left(\frac{\delta^2}{M}\right)}{4N_0}\right)^{-M}\right). \quad (13)$$

In deriving (13), we have implicitly used the *bit-error uniform property*, i.e., that the error properties of the coded sequence depend only on the weights, rather than the distances (or locations) of the nonzero symbols in the error events. This property holds true for our PEP upper bound in (13), under the simplifying approximations A1–A3.

The upper bound in (13) manifests a *multiplicative diversity* effect: The slope of the error rate curve at high SNR is Md_{free}. A convolutionally coded (or in general EC-coded) transmission without unitary precoding will have a performance upper bound given by (13) with $M = 1$, simply because it can be viewed as a joint coded–precoded transmission with precoder size $M = 1$.

We will denote an EC-coded transmission with (respectively, without) unitary precoding by EC-UP (EC-only). When OFDM modulation is used, we use the terms EC-UP-OFDM and EC-OFDM, respectively. When the code is convolutional (respectively, turbo), "EC" will be replaced by "CC" ("TC").

For $M \geq 2$, the gain in SNR of an EC-UP system as compared to an EC-only system can be evaluated from (13) by equating the argument of the $B(\cdot)$ function in (13) with $(1+\delta_0^2/4N_0)^{-1}$, where δ_0 is the minimum constellation distance needed for the EC-only system to achieve the same performance as the EC-UP system. The ratio $G_{\text{up}} := \delta_0^2/\delta^2$ measures the gain in SNR introduced by precoding. It can be readily found to be

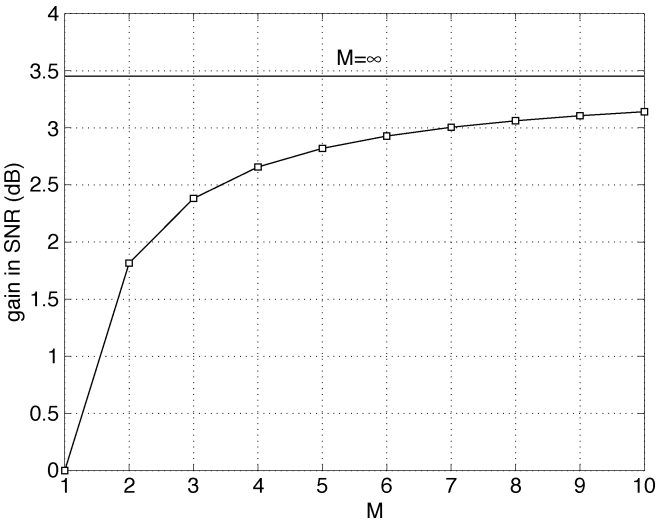

Fig. 2. Gain of unitary precoding at SNR $= 8$ dB as a function of the precoder size M.

$$G_{\text{up}} = \frac{\delta_0^2}{4N_0M\left[\left(1+\frac{\delta_0^2}{4N_0}\right)^{\frac{1}{M}}-1\right]} \overset{M\to\infty}{\longrightarrow} \frac{\frac{\delta_0^2}{(4N_0)}}{\ln\left(1+\frac{\delta_0^2}{(4N_0)}\right)}. \quad (14)$$

The gain is monotonically increasing with M. For a BPSK constellation with a rate 1/2 CC, $\delta = 2\sqrt{E_s} = \sqrt{2E_b}$, we show in Fig. 2 the gain G_{up} at $E_b/N_0 = 8$ dB of the EC-UP system, or $\delta_0^2 = 12.6N_0$. Notice that the gain for $M = 4$ is already quite large (2.7 dB). Further increasing M results in no more than 0.8-dB gain in SNR, because the ultimate gain with $M = \infty$ is about 3.5 dB.

Example 1: Consider a rate 1/2 CC with generators (133, 171) as the one used in the HiperLan/2 standard [11], BPSK constellation, and precoder size $M = 4$ [e.g., the second one in (5)]. For BPSK, we have $\delta = 2\sqrt{E_s} = \sqrt{2E_b}$. The code has $d_{\text{free}} = 10$ and $B(Z) = 36Z^{10} + 211Z^{12} + 1404Z^{14} + 11\,633Z^{16} + \ldots$, which are obtained using the transfer function method as in [1, p. 544]. Under the perfect interleaving conditions A1 and A3, the BER can then be upper bounded by $P_b \leq (1/2)B([1+E_b/(8N_0)]^{-4})$.

Using the following puncturing matrix:

$$P_{\frac{3}{4}} = \begin{bmatrix}1 & 1 & 0\\ 1 & 0 & 1\end{bmatrix} \quad (15)$$

we can obtain a punctured code of rate 3/4 from the rate 1/2 code, having $d_{\text{free}} = 5$ and $B_{3/4}(Z) = (42Z^5 + 201Z^6 + 1492Z^7 + 10\,469Z^8 + \ldots)/3$. We depict the performance upper bound (13) for these rate 1/2 and 3/4 codes with $M = 1, 2, 4$, in Fig. 3. The $M = 1$ curves correspond to convolutionally coded systems without precoding. We can observe from the slope of the curves that there is a multiplicative diversity gain introduced by precoding. Also, the gains at SNR $= 8$ dB of the rate 1/2 CC check with those of Fig. 2.

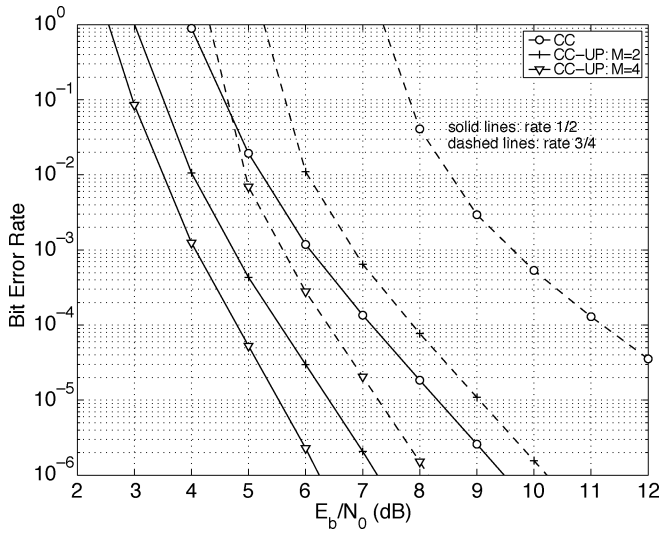

Fig. 3. Comparison between convolutionally coded systems with and without precoding.

Remark 1: We have used the fact that $|\Delta s_{n_a}| \geq \delta$ in getting (11) from (10). This corresponds to the worst-case analysis (see, e.g., [18]). A more elaborate analysis may give tighter bounds.

Remark 2: A tighter bound than the one in (12) can be derived in closed integral form [23]

$$P_2(w) \leq \frac{1}{\pi} \int_0^{\frac{\pi}{2}} \left(1 + \frac{\frac{\delta^2}{M}}{4N_0 \sin^2 \theta} \right)^{-wM} d\theta \qquad (16)$$

where $P(\tilde{\mathbf{c}} \rightarrow \mathbf{c})$ in (12) has been made an explicit function $P_2(w)$ of the weight w. Using this bound, the BER of the system can be written as $P_e \leq \sum_{w=d_{\text{free}}}^{\infty} B_w P_2(w)$. This new upper bound is about 1 dB tighter for the systems in Example 1.

Remark 3: In two places we have relied on perfect interleaving: 1) in assuming that α_j's are independent indentically distributed and 2) in assuming that $s_{n_a}, a \in [1, w]$, are precoded by different precoders. Random interleavers approximately satisfy both of these assumptions. The larger the interleavers' size, the more plausible these assumptions become. Certainly, the degree of channel variation affects how correlated α_j's are. In practice, where perfect interleaving is impossible, the performance is going to be worse than the idealized case analyzed here. Analysis with nonideal interleavers is possible using more involved methods such as those in [15], but we will not pursue them here. Instead, we will only test channel correlation effects via simulations. For the second assumption, since the performance is dominated by low weight error events, the accuracy loss incurred is small, and the approximation is practically valid.

We conclude this section by summarizing the results in the following proposition.

Proposition 1: Under the conditions of 1) perfect interleaving and 2) full diversity LP with equal amplitude precoder entries, a jointly coded–precoded system exhibits performance upper bounded by (13); or, more tightly, by $\sum_{w=d_{\text{free}}}^{\infty} B_w P_2(w)$ with $P_2(w)$ given by (16), where $B(Z) = \sum_{w=d_{\text{free}}}^{\infty} B_w Z^w$ is the bit-error enumerating function of the EC code, M is the precoder size, and d_{free} is the free distance of the code (replace d_{free} by $d_{\min}$ if a block code is used). The diversity order of the system is, therefore, Md_{free}. The gain in SNR offered by LP is quantified in (14).

C. Discussion on the Interleaver Design

The two interleavers (Π_1 and Π_2) in our system serve different purposes. Interleaver Π_1 is mainly used to separate the coded bits so that neighboring bits are mapped to different constellation symbols and, finally, precoded into different blocks. The main role of interleaver Π_2 on the other hand, is to permute each block of linearly precoded symbols in the frequency domain. At least one of the two interleavers should be large enough so that the correlation of the channel taps in the time domain can be decreased to render the model in (2) valid. In the simulations, we will select the size Π_2 equal to the OFDM symbol size N (the number of subcarriers), and choose Π_1 to have size $\gg N$.

From our PEP analysis in Section III-A, we realize that it is important to spread the consecutive input bits by at least M in the interleaver output. In this respect, block interleavers are better than random interleavers. But it is also important to avoid systematic patterns in the interleaver. Existing interleaver designs for TCs are also applicable to our setup [7], [8], [22]. For simplicity, however, we will use random interleavers in our simulations.

IV. Turbo Decoding

An exhaustive search over all possible input sequences certainly offers exact ML detection for our joint coded–precoded transmissions. The presence of the interleaver Π_1, in between the EC code and the linear precoder, prevents application of most efficient ML decoders to our joint detection problem. However, it has been widely demonstrated that iterative (turbo) decoding is quite effective in dealing with such joint ML detection problems. In this section, we will show how the turbo principle applies to our joint UP decoding and EC decoding problem.

A. Turbo Principle for Joint Coding–Precoding

The turbo principle [3] amounts to passing soft information between two maximum *a posteriori* (MAP) soft-input soft-output (SISO) modules [2], iteratively. Other approximate MAP modules, such as Max-Log MAP, modified soft-output Viterbi algorithm (SOVA), etc., can also be used [27]. We will only consider bit-wise MAP decoding in this paper. When the constellation is multilevel iterative bit demapping can also be used [24]. The soft information can be in the form of likelihood, log-likelihood ratios (LLRs), or just the probability distribution of an encoder's input and output symbols.

Each SISO module is a four-port device that accepts as input the probability distribution of both the input and the output of a coder (or a UP), and outputs an updated probability distribution of both the input and the output, based on the module's input distribution and the coder (or precoder) structure. To decode our coded–precoded transmission, we need two SISO modules that we denote as SISO-LP and SISO-EC in Fig. 4.

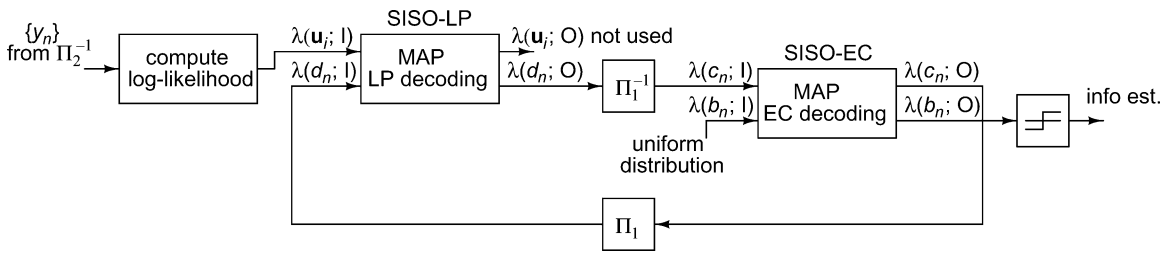

Fig. 4. Decoding diagram with SISO modules.

Inputs and outputs of the SISO modules are in the form of LLRs, denoted by $\lambda(\cdot; I)$ for inputs, and $\lambda(\cdot; O)$ for outputs. For example

$$\lambda(d_n; I) = \log \frac{P[d_n = +1; I]}{P[d_n = -1; I]} \tag{17}$$

$$\lambda(\mathbf{u}_i; I)|_{\mathbf{u}_i = \mathbf{u}} = \log \frac{P[\mathbf{u}_i = \mathbf{u}; I]}{P[\mathbf{u}_i = \mathbf{v}; I]}, \qquad \mathbf{u} \in \mathcal{U} \tag{18}$$

where in defining $\lambda(\mathbf{u}_i; \mathbf{I})$, we can use any fixed $\mathbf{v} \in \mathcal{U}$ as a reference.

The output of each SISO module will be interleaved (or deinterleaved) to be used as input to the other module. The decoding algorithm can be described as in Algorithm 1.

Algorithm 1 The iterative (turbo) decoding algorithm

S1) Obtain $\{y_n\}$ from OFDM demodulation and deinterleaver Π_2^{-1}.
S2) Compute the LLR of $\{\lambda(\mathbf{u}_i; I)\}$.
S3) Set both $\lambda(d_n; I)$ and $\lambda(b_n; I)$ to zero, $\forall n$.

Begin iterative decoding

S4) Execute the SISO-LP module to produce $\{\lambda(d_n; O)\}$.
S5) Deinterleave $\{\lambda(d_n; O)\}$ to obtain $\lambda(c_n; I)$.
S6) Execute the SISO-EC module to produce $\{\lambda(c_n; O)\}$ and $\{\lambda(b_n; O)\}$.
S7) Interleave $\{\lambda(c_n; O)\}$ to obtain $\{\lambda(\mathbf{u}_i; I)\}$. If the number of iterations is less than a maximum number allowed, then go to S4. Otherwise, go to the next step.

End iterative decoding

S8) Compare $\lambda(b_n; O)$ with zero, and output the decisions.

Next, we describe our two SISO modules in detail. We will first describe the SISO-LP module, and evaluate the computations needed in S2. Then we will describe briefly the SISO-EC module and detail the complexity of the entire turbo-decoding algorithm.

B. SISO-LP Module

The SISO-LP module implements MAP decoding of the constellation mapped and linearly precoded symbols. With reference to Fig. 4, the SISO-LP module outputs the *extrinsic information* [2], [3] $\{\lambda(\mathbf{u}_i; O)\}$ and $\{\lambda(d_n; O)\}$, using as input the *a priori* information $\{\lambda(\mathbf{u}_n; I)\}$ and $\{\lambda(d_n; I)\}$. The extrinsic information of a symbol (or symbol vector) is its LLR given other symbols' (or symbol vectors') prior information, along with the structure of the precoder. In our case, the outputs $\{\lambda(\mathbf{u}_i; O)\}$ are not used; hence, we only need to evaluate $\lambda(d_n; O)$, which is the LLR of d_n given $\{d_k : k \neq n\}$'s, priors $\{\lambda(d_k; I) : k \neq n\}$, and the priors $\{\lambda(\mathbf{u}_i; I)\}$

$$\begin{aligned}\lambda(d_n; O) &= \log \frac{P\left[d_n = +1 | \{\lambda(d_k; I) : k \neq n\}, \{\lambda(\mathbf{u}_i; I)\}\right]}{P\left[d_n = -1 | \{\lambda(d_k; I) : k \neq n\}, \{\lambda(\mathbf{u}_i; I)\}\right]} \\ &= \underbrace{\log \frac{P\left[d_n = +1 | \{\lambda(d_k; I)\}, \{\lambda(\mathbf{u}_i; I)\}\right]}{P\left[d_n = -1 | \{\lambda(d_k; I)\}, \{\lambda(\mathbf{u}_i; I)\}\right]}}_{:= \Lambda(d_n; O)} \\ &\quad - \lambda(d_n; I)\end{aligned} \tag{19}$$

where $\Lambda(d_n; O)$ is the complete *a posteriori* probability (APP) of d_n, and the equation follows from the definition of conditional probability. We next describe how to compute $\Lambda(d_n; O)$, which can then be used in (19) to compute $\lambda(d_n; O)$. The computations are similar to the those involved in the soft multiuser detection in [29], with two exceptions: 1) instead of multiuser spreading codes here we have LP, and 2) we allow for non-BPSK as well as BPSK constellations.

From (2), we know that $(P(y_n|u_n) = 1/(\pi N_0) \exp(-|y_n - \alpha_n u_n|^2/N_0)$. Thus, we can compute $P(\mathbf{u}_i = \mathbf{u}; I) := P(\mathbf{u}_i = \mathbf{u}|\{y_n\})$ as

$$\begin{aligned}&P(\mathbf{u}_i = \mathbf{u}; I) \\ &\quad = \frac{P(\mathbf{u}_i = \mathbf{u})}{P(y_{iM}, \ldots, y_{iM+M-1})} \\ &\qquad \times \prod_{m=0}^{M-1} P\left(y_{iM+m} | u_{iM+m} = [\mathbf{u}]_m\right) \\ &\quad = C \prod_{m=0}^{M-1} \exp\left(-\frac{\left|y_{iM+m} - \alpha_{iM+m}[\mathbf{u}]_m\right|^2}{N_0}\right)\end{aligned} \tag{20}$$

where C is a constant irrelevant to the computation of the LLRs, and we have assumed the *a priori* probabilities $P(\mathbf{u}_i = \mathbf{u})$ are

all equal to $1/|\mathcal{U}|$ for any $\mathbf{u} \in \mathcal{U}$. Then, the LLR of $\mathbf{u}_i$ can be obtained by definition as

$$\lambda(\mathbf{u}_i = \mathbf{u}; I) = \sum_{m=0}^{M-1} \left(-\frac{|y_{iM+m} - \alpha_{iM+m}[\mathbf{u}]_m|^2}{N_0} \right) - C'$$

where $C' := \log \lambda(\mathbf{u}_i = \mathbf{v}; I)$ is a constant that will be canceled out eventually and can be set to zero for simplicity. This accomplishes the step S2 of the decoding algorithm.

We know that each coded bit will be mapped to a constellation symbol, say s_n, together with other coded bits if the constellation size is larger than two. We denote the constellation size by Q. Each constellation symbol will be precoded together with $M-1$ other symbols to produce one precoded block $\mathbf{u}_i$. Let us denote by $\mathcal{I}_i$ the set of indexes of coded bits $\{d_n\}$ that are precoded to form $\mathbf{u}_i$; $\mathcal{I}_i$ consists of a sequence of $B := M \log_2 Q$ consecutive integers. If BPSK is used, then $\mathcal{I} = [iM, iM + M - 1]$. For any $l \in \mathcal{I}_i$, we define $\mathcal{U}_l^1$ to be the subset of $\mathcal{U}$ that corresponds to $d_l = 1$, and similarly $\mathcal{U}_l^0$ to be the subset that corresponds to $d_l = 0$. The complete APP $\Lambda(d_l; O)$ for the coded bit d_l can then be computed from (21), where $\mathbf{u}$ is the result of constellation mapping and precoding of $\{d_l : l \in \mathcal{I}_i\}$, and we have used the definitions in (17) and (18), and the fact that $P(d_l; I) = (1/2)[1 + d_l \tanh((1/2)\lambda(d_l; I))]$ (see, e.g., [29]). Once $\Lambda(d_l; O)$ is obtained, we can use (19) to obtain $\lambda(d_n; O)$, which completes step S4 of the decoding algorithm, as shown in (21) at the bottom of the page.

C. SISO-EC Module

The SISO-EC module obviously depends on the EC code used. For CCs, the soft information $\lambda(c_n; O)$ and $\lambda(b_n; O)$ can be obtained by optimum or suboptimum SISO decoding algorithms, including the Bahl–Cocke–Jelinek–Raviv (BCJR) algorithm, the SOVA, Log-MAP, or max-Log-MAP alternatives [27]. Among them, BCJR and Log-MAP are optimum decoders. The complexity of Log-MAP is lower than that of BCJR, and is approximately four times that of Viterbi's algorithm [25].

When a TC is used as the EC code, each execution of the SISO-EC module will correspond to a few TC iterations. The soft output information from the turbo decoder for the TC, will be used in step S4 of the global iteration in Algorithm 1. Since otherwise our SISO-EC module is similar to existing ones (see, e.g., [2]), we will not elaborate on it any further.

D. Complexity

In this subsection, we analyze the arithmetic complexity of the decoding algorithm in terms of approximate number of flops. We do not consider the finite word-length effects and the associated complexity issues. We refer the interested readers to [17], which deals with precision issues of TCs.

We also ignore the complexity introduced by the interleavers. But we remark that in very large scale integration implementations, the interleavers' size is limited by the memory requirements of the interleavers. "Per bit" in this subsection will mean the same thing as "per coded bit." Recall that Q is the constellation size and B is the number of bits in each precoded block: $B = M \log_2 Q$. We will consider the complexity per bit taking into account the following stages:

1) The OFDM demodulation involves only FFT processing, which has a per constellation symbol complexity of $\log_2(N)$ flops, where N is the FFT size; the complexity per bit is, thus, $\log_2(N)/\log_2(Q)$.
2) To obtain $\lambda(\mathbf{u}_i; I)$ from (20), we need $4M$ flops (we count one addition and one multiplication as two flops) for each $\mathbf{u} \in \mathcal{U}$, for a total of $Q^M \cdot 4M$ per B bits. The number of flops per bit is $4Q^M/\log_2 Q$.
3) To compute $\lambda(d_l; O)$ from (19) and (21) in the SISO-LP module, we need about $3B \cdot Q^M$ flops per bit times the number of iterations involved.
4) The complexity of obtaining $\lambda(b_n; O)$ and $\lambda(c_n; O)$ in the SISO-EC module depends on the code used. For CCs, the complexity per bit is proportional to the number of trellis states. For HiperLan, the CC has 64 states. This implies that the complexity per bit will be a few (say eight—a factor of two from the add-compare-select operation and a factor of four for the Log-MAP algorithm as a generalized Viterbi algorithm [25]) times 64 flops. We denote the number flops per bit needed in the SISO-EC by F_{EC}. This has to be multiplied by the number of iterations.

If we denote the number of iterations by N_{iter}, then summing up the number of flops we find that per bit we need about

$$\frac{\log(N)}{\log_2 Q} + \frac{4Q^M}{\log_2(Q)} + N_{\mathrm{iter}}(3BQ^M + F_{\mathrm{EC}}) \approx N_{\mathrm{iter}}(3BQ^M + F_{\mathrm{EC}})$$

flops. A typical value for N_{iter} is three.

For example, if BPSK constellation is used with a precoder of size $M = 4$, then $Q = 2$ and $B = M \log_2 Q = M = 4$. So, $3BQ^M = 198$, about three times the number of states in the trellis. Considering the HiperLan code, which gives $F_{\mathrm{EC}} \approx 64 \times 8 = 512$, the overall complexity of the system is about four times that of a CC-only HiperLan, if $N_{\mathrm{iter}} = 3$. To achieve the same amount of diversity increase, i.e., from $d_{\mathrm{free}} = 9$ to $Md_{\mathrm{free}} = 36$ by convolutional coding alone, the code memory

$$\begin{aligned}\Lambda(d_l; O) &= \log \frac{\sum_{\mathbf{u} \in \mathcal{U}_l^1} P(\mathbf{u}_i = \mathbf{u}; I) \prod_{l \in \mathcal{I}_l} P(d_l; I)}{\sum_{\mathbf{u} \in \mathcal{U}_l^0} P(\mathbf{u}_i = \mathbf{u}; I) \prod_{l \in \mathcal{I}_l} P(d_l; I)} \\ &= \log \frac{\sum_{\mathbf{u} \in \mathcal{U}_l^1} \left\{ \exp[\lambda(\mathbf{u}_i = \mathbf{u}; I)] \prod_{l \in \mathcal{I}_l} \left[1 + d_l \tanh\left(\frac{1}{2}\lambda(d_l; I)\right)\right] \right\}}{\sum_{\mathbf{u} \in \mathcal{U}_l^0} \left\{ \exp[\lambda(\mathbf{u}_i = \mathbf{u}; I)] \prod_{l \in \mathcal{I}_l} \left[1 + d_l \tanh\left(\frac{1}{2}\lambda(d_l; I)\right)\right] \right\}}\end{aligned} \tag{21}$$

would roughly need to increase $M = 4$ times from 6 to 24 [cf. (8)], and the complexity increase would be much more than the four times increase incurred by our combined coding–precoding approach.

When Q or M increases, the $3BQ^M$ term will soon dominate the complexity. In this case, the suboptimum but low-complexity instantaneous minimum mean-squared error interference cancellation algorithm of [29] can be used instead of the exhaustive ML search in the SISO-LP module; its complexity is M^2 per bit, much lower than the ML enumeration.

V. Simulation Results

In this section, we simulate our system with EC coding and LP. The precoder size will be $M = 4$ whenever LP is present. In all simulations, the BPSK constellation is used for simplicity. The simulation is run for each SNR until either 30 frame (a frame has the same size as the larger size of interleavers Π_1 and Π_2) errors are collected or 1000 frames have been sent, whichever occurs earlier.

Test Case 1 (*CC-UP with perfect interleaving*) We simulated the performance of a perfectly interleaved OFDM system as modeled in (2), which can also be viewed as transmitting directly through a flat-fading channel without using OFDM. We compared the performance of CC-only against CC-UP. The CC used is the rate 3/4 code of Example 1, which is also the code used in HiperLan/2. We decoded the CC-UP based on our iterative algorithm of Section IV. For CC-only, Viterbi decoding is used. It can be seen from Fig. 5 that the iterative decoding algorithm virtually converges after only two iterations. And the gain due to LP is significant (about 5 dB at BER $= 10^{-4}$). The performance bound in (16) is also depicted with dashed lines, and agrees with the simulation results up to less than 1-dB difference at high SNR. The bounds in Fig. 3 are looser than the ones shown in Fig. 5 by about one more decibel. The price paid for the considerably improved performance is higher complexity (about four times with two iterations).

Test Case 2 (*CC-UP-OFDM with a HiperLan/2 channel*) We depict in Fig. 6 the simulated performance of CC-UP-OFDM in a setup mimicking HiperLan/2 with Channel Model B [10]. The OFDM symbol size (i.e., the FFT/IFFT size) is 64. The delay of each channel tap is rounded up to the nearest symbol so that we have 16 symbol-spaced taps. The taps are independent complex Gaussian random variables, with variances given in the tap order by (0.26, 0.244, 0.224, 0.0707, 0.0793, 0.0478,0.0295, 0.0178, 0.0107, 0.006 45, 0.005 01, 0.002 51, 0, 0.001 48, 0, 0.000 602). The channel is assumed to remain constant during one OFDM symbol period, and each tap varies from one OFDM symbol to the next according to Jakes' model. The carrier frequency is 5.2 GHz, and the mobile's velocity is 3 m/s. The interleaver Π_2 is a block interleaver of size 16×4 so that each precoded block is maximally spread out in the frequency domain. The interleaver Π_1 is chosen to be a random interleaver of size corresponding to 256 OFDM symbols. The delay of the system due to interleaving is, therefore, about 1 ms in HiperLan/2.

The performance of CC-OFDM with a random interleaver of the same size is also depicted in the same figure. It can be seen that with either interleaver, CC-UP-OFDM outperforms

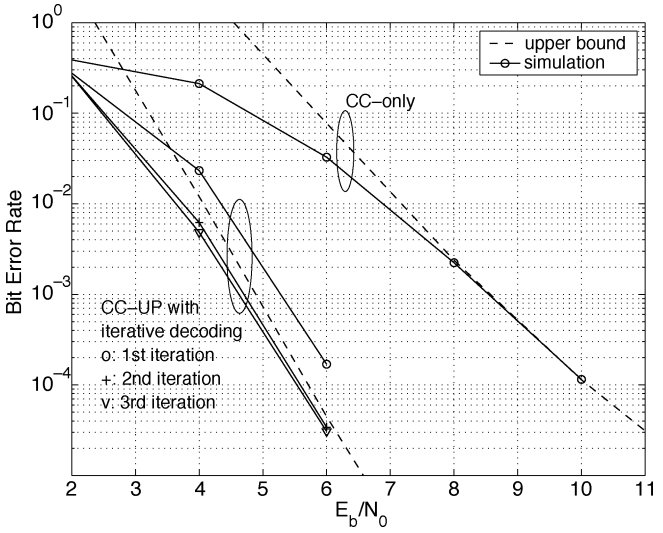

Fig. 5. Simulations (solid lines) comparing CC-UP with $M = 4$ and CC-only in perfectly interleaved channels, together with the analytical upper bounds (dashed lines).

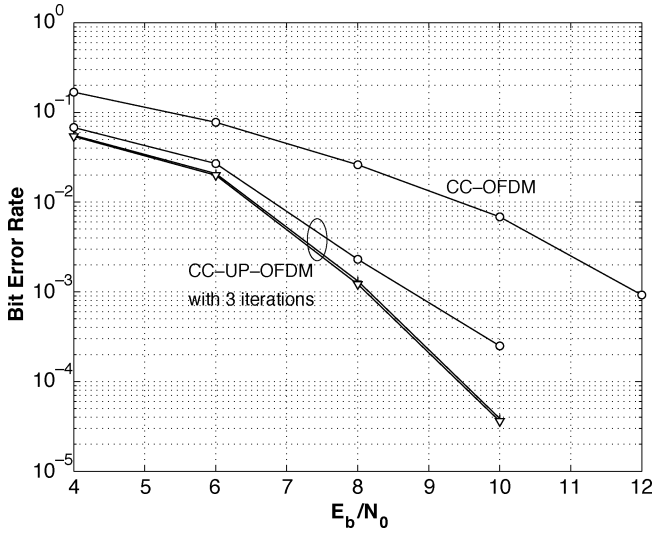

Fig. 6. CC-UP-OFDM with $M = 4$ in HiperLan channels with random interleaver.

CC-OFDM, at the price of higher complexity, even with only one iteration. The random interleaver performs better for SNR >6 dB. CC-UP-OFDM with a random interleaver outperforms the standard CC-OFDM by about 4 dB at BER $= 10^{-3}$ with only three iterations. Comparison with the results in Test Case 1 illustrates that the channel correlation indeed lowers the system performance, as expected.

Test Case 3 (*Turbo-coded transmissions*) In this simulation, we replace the CC of the previous simulation by a TC, while maintaining the same simulation setup. The main purpose is to show that even turbo-coded OFDM transmissions can benefit from LP. We compare TC-UP-OFDM and TC-OFDM using the TC with constituent code [1 35/23], punctured to rate 3/4 by keeping the systematic bits and every $(6n-1)$th parity bit from the first constituent code, and every $(6n)$th parity bit from the second constituent code, $n = 1, 2, \ldots$. The result is reported in Fig. 7. Each iteration consists of one iteration between

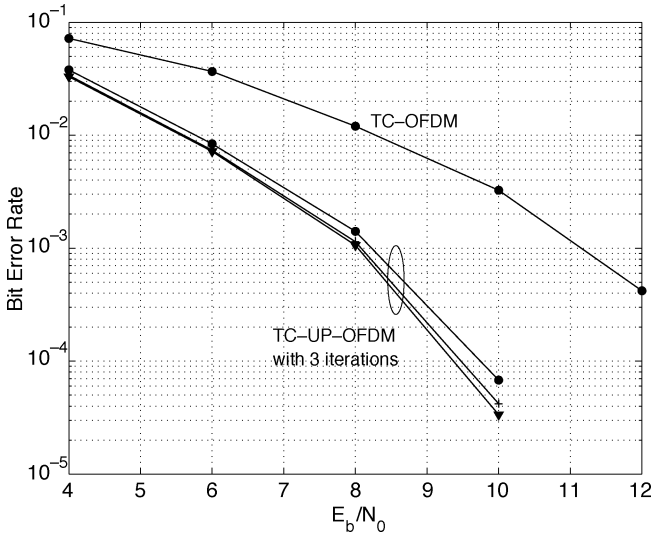

Fig. 7. TC-UP-OFDM with $M = 4$ and random interleaver in HiperLan channels.

the SISO-LP module and SISO-EC module; within SISO-EC module, three inner-iterations are used for the TC decoding. We observe that although TC-OFDM also benefits from iterative decoding, there is about 4-dB gain at 10^{-3} achieved by the LP after three iterations. We notice that for the simulated setup, one iteration between SISO-LP and SISO-EC is enough.

VI. Conclusion and Discussion

We have proposed joint EC coding and LP for fading-resilient transmissions over frequency-flat and frequency-selective fading channels encountered with high-rate wireless OFDM transmissions. Through upper bound analysis, we quantified the gain in SNR offered by introducing LP to coded transmissions. The combination offers a multiplicative benefit to the achievable diversity: The overall diversity is the $d_{\min}$ of the EC code multiplied by the precoder size. An iterative decoding algorithm was derived for low-complexity turbo decoding. The complexity increase turned out to be only a few times that of a coded transmission without precoding. The same amount of diversity increase would lead to a much higher increase in decoding complexity, if EC coding is to be used alone. Extensive simulations verified the superior performance of joint coding–precoding for both simulated, and practical HiperLan/2 channels. Other applications of the proposed schemes include digital video broadcasting [9], [20]. Since the proposed scheme modifies the transmitter design, backward compatibility becomes an issue; it is, therefore, more suitable for future generation wireless communications.

References

[1] S. Benedetto and E. Biglieri, *Principles of Digital Transmission With Wireless Applications*. New York: Kluwer/Plenum Publishers, 1999.

[2] S. Benedetto, G. Montorsi, D. Divsalar, and F. Pollara. (1996, Nov.) A Soft-Input Soft-Output Maximum A Posterior (MAP) Module to Decode Parallel and Serial Concatenated Codes, NASA JPL TDA Progress Report. [Online]Available: http://tmo.jpl.nasa.gov/tmo/

[3] C. Berrou, A. Glavieux, and P. Thitimajshima, "Near Shannon limit error-correcting coding and decoding: turbo codes," in *Proc. Int. Conf. Communications*, Geneva, Switzerland, May 1993, pp. 1064–1070.

[4] J. Boutros and E. Viterbo, "Signal space diversity: A power and bandwidth efficient diversity technique for the Rayleigh fading channel," *IEEE Trans. Inform. Theory*, vol. 44, pp. 1453–1467, July 1998.

[5] D. Dardari and V. Tralli, "High-speed indoor wireless communications at 60 GHz with coded OFDM," *IEEE Trans. Commun.*, vol. 47, pp. 1709–1721, Nov. 1999.

[6] V. M. DaSilva and E. S. Sousa, "Fading-resistant modulation using several transmitter antennas," *IEEE Trans. Commun.*, vol. 45, pp. 1236–1244, Oct. 1997.

[7] D. Divsalar and F. Pollara. (1995, Nov.) On the Design of Turbo Codes, NASA JPL TDA Progress Report. [Online]Available: http://tmo.jpl.nasa.gov/tmo/

[8] S. Dolinar and D. Divsalar. (1995, Aug.) Weight Distributions for Turbo Codes Using Random and Nonrandom Permutations, NASA JPL TDA Progress Report. [Online]Available: http://tmo.jpl.nasa.gov/tmo/

[9] *Digital Video Broadcasting: Framing Structure, Channel Coding, and Modulation for Digital Terrestrial Television*, ETSI Standard EN 300-744, Aug. 1997.

[10] *Channel Models for HIPERLAN/2 in Different Indoor Scenarios Norme*, ETSI Standard, Document 3ERI085B, 1998.

[11] *Broadband Radio Access Networks (BRAN); HIPERLAN Type 2 Technical Specification Part 1—Physical Layer*, ETSI Standard DTS/BRAN030 003-1, Oct. 1999.

[12] B. Le Floch, M. Alard, and C. Berrou, "Coded orthogonal frequency division multiplex," *Proc. IEEE*, vol. 83, pp. 982–996, June 1995.

[13] X. Giraud, E. Boutillon, and J.-C. Belfiore, "Algebraic tools to build modulation schemes for fading channels," *IEEE Trans. Inform. Theory*, vol. 43, pp. 938–952, May 1997.

[14] R. Hoshyar, S. N. Jamali, and A. R. S. Bahai, "Turbo coding performance in OFDM packet transmissions," in *Proc. Vehicular Technology Conf.*, vol. 2, Tokyo, Japan, 2000, pp. 805–810.

[15] G. Kaplan and S. Shamai, "Achievable performance over the correlated Rician channel," *IEEE Trans. Commun.*, vol. 42, pp. 2967–2978, Nov. 1994.

[16] Z. Liu, Y. Xin, and G. B. Giannakis, "Linear constellation-precoding for OFDM with maximum multipath diversity and coding gains," *IEEE Trans. Commun.*, vol. 51, pp. 416–427, Mar. 2003.

[17] G. Montorsi and S. Benedetto, "Design of fixed-point iterative decoders for concatenated codes with interleavers," *IEEE J. Select. Areas Commun.*, vol. 19, pp. 871–882, May 2001.

[18] M. Rouanne and D. J. Costello Jr., "An algorithm for computing the distance spectrum of trellis codes," *IEEE J. Select. Areas Commun.*, vol. 7, pp. 929–940, Aug. 1989.

[19] A. Ruiz, J. M. Cioffi, and S. Kasturia, "Discrete multiple tone modulation with coset coding for the spectrally shaped channel," *IEEE Trans. Commun.*, vol. 40, pp. 1012–1029, June 1992.

[20] M. Russel and G. L. Stüber, "Terrestrial digital video broadcasting for mobile reception using OFDM," *Wireless Personal Commun.*, vol. 2, no. 1–2, pp. 45–66, 1995.

[21] H. R. Sadjadpour, "Application of turbo codes for discrete multi-tone modulation schemes," in *Proc. Int. Conf. Communications*, vol. 2, Vancouver, Canada, 1999, pp. 1022–1027.

[22] H. R. Sadjadpour, N. J. A. Sloane, M. Salehi, and G. Nebe, "Interleaver design for turbo codes," *IEEE J. Select. Areas Commun.*, vol. 19, pp. 831–837, May 2001.

[23] M. K. Simon and M.-S. Alouini, *Digital Communications Over Fading Channels: A Unified Approach to Performance Analysis*. New York: Wiley, 2000.

[24] S. ten Brink, J. Speidel, and R.-H.Ran-Hong Yan, "Iterative demapping and decoding for multilevel modulation," in *Proc. GLOBECOM*, vol. 1, 1998, pp. 579–584.

[25] A. J. Viterbi, "An intuitive justification and a simplified implementation of the MAP decoder for convolutional codes," *IEEE J. Select. Areas Commun.*, vol. 16, pp. 260–264, Feb. 1998.

[26] E. Viterbo and J. Boutros, "A universal lattice code decoder for fading channels," *IEEE Trans. Inform. Theory*, vol. 45, pp. 1639–1642, July 1999.

[27] J. Vogt, K. Koors, A. Finger, and G. Fettweis, "Comparison of different turbo decoder realizations for IMT-2000," in *Proc. GLOBECOM*, vol. 5, Rio de Janeiro, Brazil, 1999, pp. 2704–2708.

[28] H. Wang, J. Belzile, and C. L. Despins, "64-QAM OFDM with TCM coding and waveform shaping in a time-selective Rician fading channel," in *Proc. Int. Zurich Seminar Broadband Communications*, Verdun, QC, Canada, 2000, pp. 257–261.

[29] X. Wang and H. V. Poor, "Iterative (turbo) soft interference cancellation and decoding for coded CDMA," *IEEE Trans. Commun.*, vol. 46, pp. 1046–1061, July 1999.

[30] Z. Wang and G. B. Giannakis, "Wireless multicarrier communications: where Fourier meets Shannon," *IEEE Signal Processing Mag.*, vol. 47, pp. 29–48, May 2000.
[31] ——, "Complex-field coding for OFDM over fading wireless channels," *IEEE Trans. Inform. Theory*, vol. 49, pp. 707–720, Mar. 2003.
[32] S. G. Wilson, *Digital Modulation and Coding*. Englewood Cliffs, NJ: Prentice-Hall, 1996.
[33] Y. Xin, Z. Wang, and G. B. Giannakis, "Space-time diversity systems based on linear constellation precoding," *IEEE Trans. Wireless Commun.*, vol. 2, pp. 294–309, Mar. 2003.

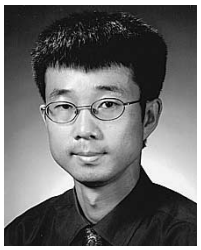

Zhengdao Wang (M'02) received the B.S. degree in electrical engineering and information science from the University of Science and Technology of China (USTC), Hefei, 1996, the M.Sc. degree in electrical and computer engineering from the University of Virginia, Charlottesville, 1999, and the Ph.D. degree in electrical and computer engineering from the University of Minnesota, Minneapolis, 2002.

He is now with the Department of Electrical and Computer Engineering at Iowa State University, Ames. His interests lie in the areas of signal processing, communications, and information theory.

Dr. Wang was the co-recipient of the IEEE Signal Processing Magazine Best Paper Award, 2003.

Shengli Zhou (M'03) received the B.S. degree and the M.Sc. degree in electrical engineering and information science from the University of Science and Technology of China (USTC), Hefei, in 1995 and 1998, respectively. He received the Ph.D. degree in electrical and computer engineering from the University of Minnesota, Minneapolis, in 2002.

He is now with the Department of Electrical and Computer Engineering at the University of Connecticut, Storrs. His research interests lie in the areas of communications and signal processing, including channel estimation and equalization, multiuser and multicarrier communications, space–time coding, adaptive modulation, and cross-layer designs.

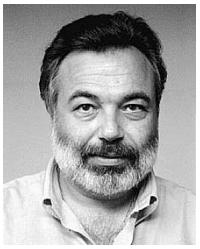

Georgios B. Giannakis (S'84–M'86–SM'91–F'97) received the Diploma in electrical engineering from the National Technical University of Athens, Greece, 1981. From September 1982 to July 1986, he was with the University of Southern California (USC), Los Angeles, where he received the M.Sc. degree in electrical engineering, the M.Sc. degree in mathematics, and the Ph.D. degree in electrical engineering, in 1983, 1986, and 1986, respectively.

After lecturing for one year at USC, he joined the University of Virginia in 1987, where he became a Professor of Electrical Engineering in 1997. Since 1999, he has been a Professor with the Department of Electrical and Computer Engineering at the University of Minnesota, Minneapolis, where he now holds an ADC Chair in Wireless Telecommunications. His general interests span the areas of communications and signal processing, estimation and detection theory, time-series analysis, and system identification—subjects on which he has published more than 190 journal papers, 350 conference papers, and two edited books. Current research focuses on transmitter and receiver diversity techniques for single-user and multiuser fading communication channels, complex-field and space–time coding, multicarrier, ultrawideband wireless communication systems, cross-layer designs, and distributed sensor networks.

Dr. Giannakis is the (co-) recipient of five best paper awards from the IEEE Signal Processing (SP) Society (1992, 1998, 2000, 2001, 2003). He also received the Society's Technical Achievement Award in 2000. He served as Editor in Chief for the IEEE SIGNAL PROCESSING LETTERS, as Associate Editor for the IEEE TRANSACTIONS ON SIGNAL PROCESSING and the IEEE SIGNAL PROCESSING LETTERS, as Secretary of the SP Conference Board, as Member of the SP Publications Board, as Member and Vice-Chair of the Statistical Signal and Array Processing Committee, as Chair of the SP for Communications Technical Committee, and as a Member of the IEEE Fellows Election Committee. He has also served as a Member of the IEEE-SP Society's Board of Governors, the Editorial Board for the PROCEEDINGS OF THE IEEE, and the Steering Committe of the IEEE TRANSACTIONS ON WIRELESS COMMUNICATIONS.